

## COMMUNICATION

View Article Online  
View Journal | View IssueCite this: *Dalton Trans.*, 2024, **53**, 13326Received 27th June 2024,  
Accepted 25th July 2024

DOI: 10.1039/d4dt01424c

rsc.li/dalton

Superionic conduction in a Mg<sup>2+</sup>-containing covalent organic framework at intermediate temperature†

Akinori Mohri, Yuki Oami and Masaaki Sadakiyo \*

We report superionic conduction in a Mg<sup>2+</sup>-containing covalent organic framework (COF) at intermediate temperature in the absence of guest vapors. A COF containing Mg<sup>2+</sup> carriers and polyethylene oxide (PEO) chains in its channels (TPB-PEO-9-COF-Mg) was synthesized. TPB-PEO-9-COF-Mg showed superionic conductivity above 10<sup>-4</sup> S cm<sup>-1</sup> under dry N<sub>2</sub> at 160 °C.

Magnesium ion (Mg<sup>2+</sup>) conduction in solids is a current topic in materials chemistry because of its potential application as an electrolyte in rare-element-free secondary batteries.<sup>1</sup> However, it is known that the divalency of Mg<sup>2+</sup> prevents its migration in solids because of the strong electrostatic interaction with neighboring anions.<sup>2</sup> So far, to enhance the ionic conductivity of Mg<sup>2+</sup>, two approaches have been mainly studied in traditional solids having closely-packed structures. One is to reduce the electrostatic interaction by increasing the ionic radius of the neighboring anions by employing S<sup>2-</sup> or Se<sup>2-</sup> instead of O<sup>2-</sup>, which led to superionic conductivity of around 10<sup>-4</sup> S cm<sup>-1</sup> (*i.e.*, MgSc<sub>2</sub>Se<sub>4</sub>) at ambient temperature (25 °C).<sup>3</sup> Another is to elevate the operating temperature by employing thermally stable materials, which led to superionic conductivity above 10<sup>-4</sup> S cm<sup>-1</sup> (*e.g.*, MgZr<sub>4</sub>(PO<sub>4</sub>)<sub>6</sub>) at high temperature (>500 °C).<sup>2,4</sup> However, there is a lack of an effective approach to realize such superionic conductivity (>10<sup>-4</sup> S cm<sup>-1</sup>) of Mg<sup>2+</sup>-containing materials in the temperature region between them, which is sometimes called the intermediate temperature region (*e.g.*, 100–300 °C).<sup>5</sup>

Recently, crystalline porous solids such as metal–organic frameworks (MOFs) and covalent organic frameworks (COFs) have emerged as a new class of ionic conductors.<sup>6</sup> Regarding Mg<sup>2+</sup> conduction, we recently reported that Mg<sup>2+</sup>-containing MOFs show superionic conductivity above 10<sup>-4</sup> S cm<sup>-1</sup> at low

temperature (25 °C) in the presence of vapors of small guest molecules such as MeCN.<sup>7–9</sup> We found that the adsorbed guest molecules in the MOF's pores accelerate the migration of Mg<sup>2+</sup> through the formation of coordinated Mg<sup>2+</sup> carriers, which would reduce the electrostatic interaction with neighboring species.<sup>8</sup> However, one of the problems is that the high ionic conductivity is only present in the presence of guest vapors, and thus the operating temperature is limited at least below boiling points of small guest molecules (*e.g.*, ≲82 °C for MeCN). On the other hand, some COFs including polyethylene oxide (PEO) chains in their channels have recently been reported as guest-molecule-free ionic conductors operating in the intermediate temperature region.<sup>10–12</sup> However, all the cases dealt with Li<sup>+</sup> conduction which is enhanced by segmental motion of the included PEO chains and there is no report of Mg<sup>2+</sup>-conducting COFs.

Here, we report on superionic conduction in a Mg<sup>2+</sup>-containing COF in the absence of guest vapors. According to the case of Li<sup>+</sup>-conducting COFs,<sup>10–12</sup> we employed long PEO chains (PEO-9, Fig. 1) to achieve high ionic conductivity in the intermediate temperature region without the presence of small guest molecules. The long PEO chains were introduced in the channels of a COF (TPB-PEO-9-COF) to help the migration of the included Mg<sup>2+</sup> through their segmental motion. The COF

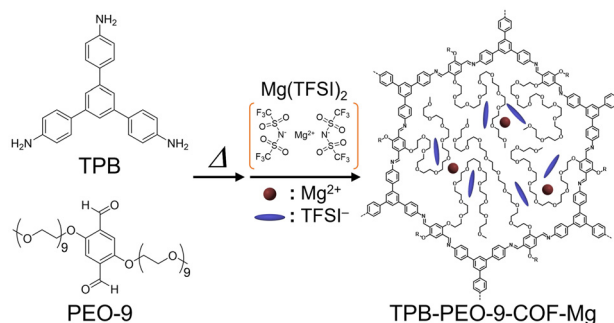


Fig. 1 Schematic illustration of the synthesis of TPB-PEO-9-COF-Mg.

Department of Applied Chemistry, Faculty of Science Division I, Tokyo University of Science, 1-3 Kagurazaka, Shinjuku-ku, Tokyo 162-8601, Japan.

E-mail: sadakiyo@rs.tus.ac.jp

† Electronic supplementary information (ESI) available: Details of synthesis and physical measurements; Nyquist plots; dc polarization curve; list of activation energies; XRPD patterns. See DOI: <https://doi.org/10.1039/d4dt01424c>

containing long PEO chains and  $\text{Mg}^{2+}$  carriers (TPB-PEO-9-COF-Mg) was synthesized by introduction of  $\text{Mg}(\text{TFSI})_2$  ( $\text{TFSI}^- = \text{bis}(\text{trifluoromethanesulfonyl})\text{imide}$ ) after the imination reaction with 1,3,5-tri(4-aminophenyl)benzene (TPB) and 2,5-bis(nonaethylene glycol)oxy-1,4-dibenzaldehyde (PEO-9) (Fig. 1). TPB-PEO-9-COF-Mg showed superionic conductivity of  $1.8 \times 10^{-4} \text{ S cm}^{-1}$  at 160 °C under dry  $\text{N}_2$ , *i.e.*, the absence of guest vapors, which is the highest value among  $\text{Mg}^{2+}$ -containing crystalline compounds in the intermediate temperature region. Transport number of  $\text{Mg}^{2+}$  ( $t_{\text{Mg}^{2+}}$ ) was also estimated to be 0.31 and thus we could state that this is the first demonstration of a COF-based  $\text{Mg}^{2+}$  conductor.

TPB-PEO-9-COF (without  $\text{Mg}^{2+}$ ) was synthesized according to previous reports (details are shown in the ESI†).<sup>10,11</sup> TPB-PEO-9-COF was prepared by heating a mixture of TPB, PEO-9, 1,4-dioxane, mesitylene, and aqueous solution of acetic acid to form imino groups through dehydration between TPB and PEO-9. The prepared COF was characterized using X-ray powder diffraction (XRPD), infrared (IR) spectra, and elemental analysis. In the XRPD pattern (Fig. 2), the sharp peaks at around 2.76°, 5.56°, 7.40°, and 9.74° correspond to (100), (200), (210) and (220) facets, respectively,<sup>10</sup> which indicates the successful formation of the TPB-based crystalline COF.<sup>10</sup> The broadened peak at around  $\sim 21^\circ$  is attributable to the (001) facet; the significant broadening of the 001 peak is similar to that of the previously reported COF containing long PEO chains.<sup>11</sup> The good agreement between the elemental analysis (see the ESI†) and the presence of the peaks at around  $2930 \text{ cm}^{-1}$  (CH stretching vibration mode of the alkyl groups on the PEO chains) in the IR spectra (Fig. S1†) also indicated the successful synthesis of the COF. TPB-PEO-9-COF showed almost no adsorption of  $\text{N}_2$  at 77 K (Fig. S2†). Note that, as described later, we also prepared TPB-PEO-3-COF by employing PEO-3 (2,5-bis(triethylene glycol)oxy-1,4-dibenzaldehyde) and it also showed almost no adsorption of  $\text{N}_2$ . Considering the fact that the same framework with no PEO chain shows

apparent porosity,<sup>10</sup> the results indicate the presence of the PEO chains in the COF channels.

The  $\text{Mg}^{2+}$  carrier,  $\text{Mg}(\text{TFSI})_2$ , was introduced by immersing the prepared COF in tetrahydrofuran (THF) solution of  $\text{Mg}(\text{TFSI})_2$ , followed by washing with THF solvent to clean up the surface of the crystallites (see the ESI†). The amount of  $\text{Mg}^{2+}$  carriers in TPB-PEO-9-COF-Mg was 2.1 per formula (*i.e.*,  $\{\text{C}_6\text{H}_3(\text{C}_6\text{H}_4\text{N})_3\}_2\{\text{C}_6\text{H}_2(\text{C}_{38}\text{H}_{78}\text{O}_{20})(\text{CH}_2)_{23}\}_3\{\text{Mg}(\text{TFSI})_2\}_{2.1}$  (after dehydration)), determined by inductively coupled plasma atomic emission spectroscopy (ICP-AES). The incorporation of a certain amount of  $\text{Mg}^{2+}$  salt clearly indicates that TPB-PEO-9-COF has apparent capacity to include additional components, while it did not show  $\text{N}_2$  adsorption. It should be noted that we also tried to prepare a similar COF sample including  $\text{Mg}^{2+}$  with shorter PEO chains by employing PEO-3, *i.e.*, TPB-PEO-3-COF. However, TPB-PEO-3-COF did not include an apparent amount of  $\text{Mg}^{2+}$  carriers through this method. This is indicative that the long PEO chain in TPB-PEO-9-COF is critically important to accommodate the Mg salt in its channels, which would be because of the coordination ability of the PEO chain to  $\text{Mg}^{2+}$ . IR spectra of the  $\text{Mg}^{2+}$ -containing sample (Fig. 3) also confirmed the presence of the PEO chains (*e.g.*, CH stretching mode at around  $2930 \text{ cm}^{-1}$ ) and the  $\text{Mg}(\text{TFSI})_2$  salt (*e.g.*, SO stretching (at around  $1350 \text{ cm}^{-1}$ ) and CF stretching (at around  $1200 \text{ cm}^{-1}$ ) modes). The XRPD pattern of TPB-PEO-9-COF-Mg (Fig. 2) indicated apparently lower intensity of the main peaks, such as 100 (2.76°), 200 (5.56°), and 210 (7.40°), than those of TPB-PEO-9-COF, while the broadened 001 peak (at around  $\sim 21^\circ$ ) remains. There are some possibilities for this change. One is the collapse of the framework. The other is the change in electron density in the inner channels or weakening of the long-range order of the framework. To clear this point, we measured the XRPD pattern of the  $\text{Mg}^{2+}$ -desorbed sample (TPB-PEO-9-COF-recovered), prepared by immersing TPB-PEO-9-COF-Mg in THF solution of 18-crown-6-ether at RT overnight to desorb the included  $\text{Mg}^{2+}$  salt. As shown in Fig. 2, the peaks are recovered after desorption of  $\text{Mg}^{2+}$ , confirming

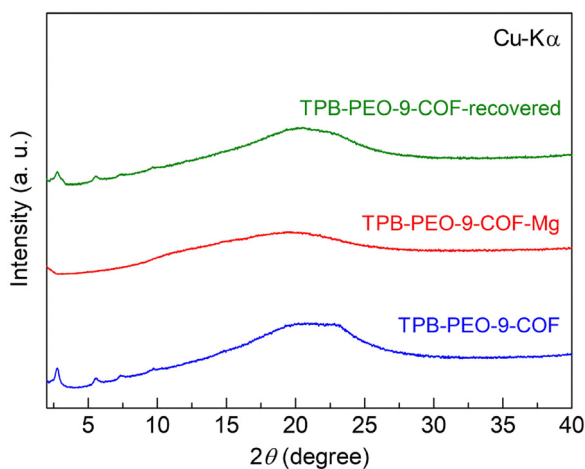


Fig. 2 XRPD patterns of (blue) TPB-PEO-9-COF, (red) TPB-PEO-9-COF-Mg, and (green) TPB-PEO-9-COF-recovered.

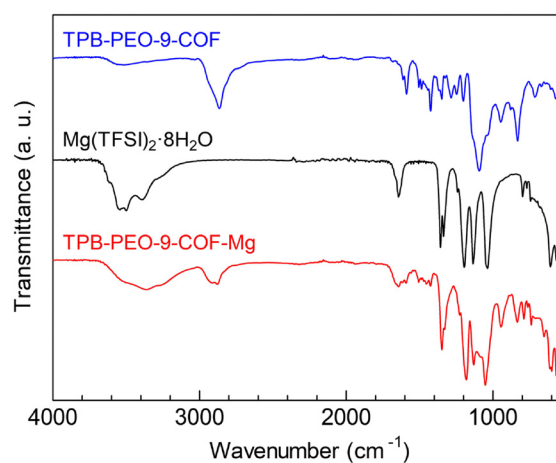


Fig. 3 IR spectra of TPB-PEO-9-COF,  $\text{Mg}(\text{TFSI})_2$  (more accurately described as  $\text{Mg}(\text{TFSI})_2 \cdot 8\text{H}_2\text{O}$  under air), and TPB-PEO-9-COF-Mg.



that the weakening of the main peaks of the  $\text{Mg}^{2+}$ -containing COF (TPB-PEO-9-COF-Mg) was not derived from the collapse of the framework and that the framework structure of the  $\text{Mg}^{2+}$ -containing sample still remains even after the  $\text{Mg}^{2+}$  incorporation.

To clarify the thermal behaviour of the samples, we performed thermogravimetry (TG) analysis and differential scanning calorimetry (DSC). As shown in Fig. S3,† the TG curves indicated that TPB-PEO-9-COF-Mg and TPB-PEO-9-COF are thermally stable below 250 °C and that some water molecules were adsorbed in the sample under air, which is consistent with the results of IR measurements (*i.e.*, presence of broad peaks at around 3200–3600  $\text{cm}^{-1}$ ). Fig. S4† shows the DSC profiles of TPB-PEO-9-COF and TPB-PEO-9-COF-Mg. As shown in Fig. S4,† these samples exhibited endothermic glass transition at around –59 °C (for TPB-PEO-9-COF) and –14 °C (for TPB-PEO-9-COF-Mg), which is similar to the case of the COFs with long PEO chains.<sup>11</sup> The difference in thermal behaviour between these samples indicated the successful incorporation of the Mg salt in the COF channels. The result also confirmed the presence of dynamic segmental motion of the PEO chains in TPB-PEO-9-COF-Mg in the temperature region above the transition, which would be critically important for efficient migration of the included ionic carriers.

To clarify the ion-conductive property of the  $\text{Mg}^{2+}$ -containing COF under the guest-vapor-free conditions, we performed alternating current (ac) impedance measurements under dry  $\text{N}_2$  (Fig. S5†). The sample was dehydrated at 130 °C (under  $\text{N}_2$  overnight) before the measurement to prevent the effect of proton conduction derived from the included water molecules under air. Fig. 4 shows the temperature dependence of the ionic conductivity of TPB-PEO-9-COF-Mg. The conductivity monotonically increased with increasing the temperature in the range from 30 to 160 °C, *i.e.*, Arrhenius-type behavior in ionic conduction. While the ionic conductivity of TPB-PEO-9-COF-Mg at ambient temperature is moderate ( $\sim 10^{-7}$   $\text{S cm}^{-1}$ ), it

gradually increases with temperature and finally reached a superionic conductivity of  $1.8 \times 10^{-4}$   $\text{S cm}^{-1}$  at 160 °C. By comparing the conductivity of TPB-PEO-9-COF (*i.e.*, without Mg (TFSI)<sub>2</sub>) and bulk Mg(TFSI)<sub>2</sub> (Fig. S6†), it is clear that this superionic conductivity is derived from the migration of Mg (TFSI)<sub>2</sub> carriers incorporated inside the COF and is not derived from some of the impurities such as bulk Mg(TFSI)<sub>2</sub> located outside the COF crystals. As described before, a superionic conductivity above  $10^{-4}$   $\text{S cm}^{-1}$  in the intermediate temperature region has not been achieved yet in  $\text{Mg}^{2+}$ -containing crystalline materials (Fig. S7†), while some superionic conductors operating in different temperature regions were reported (*e.g.*,  $(\text{Mg}_{0.1}\text{Hf}_{0.9})_{4/3.8}\text{Nb}(\text{PO}_4)_3$  ( $>10^{-4}$   $\text{S cm}^{-1}$  at 600 °C),<sup>13</sup>  $\text{MgSc}_2\text{Se}_4$  ( $\sim 10^{-4}$   $\text{S cm}^{-1}$  at 25 °C),<sup>3</sup> and  $\text{MIL-101} \supset \{\text{Mg}(\text{TFSI})_2\}_{1.6}(\text{MeCN})_n$  ( $1.9 \times 10^{-3}$   $\text{S cm}^{-1}$  at 25 °C)<sup>8</sup>). Therefore, this value (*i.e.*,  $1.8 \times 10^{-4}$   $\text{S cm}^{-1}$ ) is the highest in this temperature region. Since the migration of  $\text{Mg}^{2+}$  in TPB-PEO-9-COF-Mg cannot be demonstrated only by the ac impedance measurements because it includes both cations and anions as the ionic carriers, we measured transport number of  $\text{Mg}^{2+}$  through dc polarization of the cell composed of non-blocking electrodes (see the ESI†). As shown in Fig. S8,† steady current was successfully observed at 160 °C and the transport number of  $\text{Mg}^{2+}$  was estimated to be  $t_{\text{Mg}^{2+}} = 0.31$ , confirming the  $\text{Mg}^{2+}$  transport in the sample. Therefore, we could also state that this is the first demonstration of  $\text{Mg}^{2+}$  conduction in COFs. The activation energy at around the optimal temperature (120–160 °C) was estimated to be 0.32 eV, which is slightly higher than that of low-temperature-operating superionic conductors (*e.g.*,  $\text{MgSc}_2\text{Se}_4$ : 0.2 eV)<sup>3</sup> but apparently lower than that of high-temperature-operating superionic conductors (*e.g.*,  $\text{MgZr}_4(\text{PO}_4)_6$ : 0.87 eV),<sup>2</sup> indicating the efficient migration of the carriers in the COF channels in this temperature region.

## Conclusions

In conclusion, we demonstrated superionic conduction above  $10^{-4}$   $\text{S cm}^{-1}$  in a  $\text{Mg}^{2+}$ -containing COF in the intermediate temperature region under guest-vapor-free conditions. The PEO-containing COF, TPB-PEO-9-COF-Mg, showed a superionic conductivity of  $1.8 \times 10^{-4}$   $\text{S cm}^{-1}$  at 160 °C ( $t_{\text{Mg}^{2+}} = 0.31$ ). We clarified that the long PEO chains deeply contribute to high ionic conductivity and incorporation of  $\text{Mg}^{2+}$  carriers in the COF. These results would provide important information for the development of COF-based ionic conductors and  $\text{Mg}^{2+}$ -conductors based on such porous materials.

## Data availability

All the data used are provided in the manuscript and the ESI.†

## Conflicts of interest

There are no conflicts to declare.

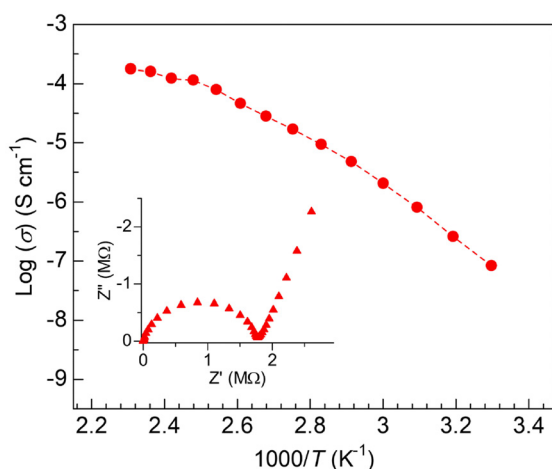


Fig. 4 Temperature dependence (30–160 °C) of ionic conductivity of TPB-PEO-9-COF-Mg under  $\text{N}_2$ . The inset shows an example of Nyquist plots (50 °C).



## Acknowledgements

This work was partly supported by the Shorai Foundation for Science and Technology, JSPS KAKENHI No. 21K05089, and JST FOREST No. JPMJFR2110.

## References

- J. Zhang, Z. Chang, Z. Zhang, A. Du, S. Dong, Z. Li, G. Li and G. Cui, Current Design Strategies for Rechargeable Magnesium-Based Batteries, *ACS Nano*, 2021, **15**, 15594–15624.
- S. Ikeda, M. Takahashi, J. Ishikawa and K. Ito, Solid Electrolytes with Multivalent Cation Conduction. 1. Conducting Species in Mg-Zr-PO<sub>4</sub> system, *Solid State Ionics*, 1987, **23**, 125–129.
- P. Canepa, S.-H. Bo, G. S. Gautam, B. Key, W. D. Richards, T. Shi, Y. Tian, Y. Wang, J. Li and G. Ceder, High magnesium mobility in ternary spinel chalcogenides, *Nat. Commun.*, 2017, **8**, 1759.
- A. Omote, S. Yotsuhashi, Y. Zenitani and Y. Yamada, High Ion Conductivity in MgHf(WO<sub>4</sub>)<sub>3</sub> Solids with Ordered Structure: 1-D Alignments of Mg<sup>2+</sup> and Hf<sup>4+</sup> Ions, *J. Am. Ceram. Soc.*, 2011, **94**, 2285–2288.
- M. Yoon, K. Suh, S. Natarajan and K. Kim, Proton Conduction in Metal–Organic Frameworks and Related Modularly Built Porous Solids, *Angew. Chem., Int. Ed.*, 2013, **52**, 2688–2700.
- M. Sadakiyo and H. Kitagawa, Ion-conductive metal–organic frameworks, *Dalton Trans.*, 2021, **50**, 5385–5397.
- Y. Yoshida, K. Kato and M. Sadakiyo, Vapor-Induced Superionic Conduction of Magnesium Ions in a Metal–Organic Framework, *J. Phys. Chem. C*, 2021, **125**, 21124–21130.
- Y. Yoshida, T. Yamada, Y. Jing, T. Toyao, K. Shimizu and M. Sadakiyo, Super Mg<sup>2+</sup> Conductivity around 10<sup>−3</sup> S cm<sup>−1</sup> Observed in a Porous Metal–Organic Framework, *J. Am. Chem. Soc.*, 2022, **144**, 8669–8675.
- K. Aoki, K. Kato and M. Sadakiyo, High Mg<sup>2+</sup> conduction in three-dimensional pores of a metal–organic framework under organic vapors, *Dalton Trans.*, 2023, **52**, 15313–15316.
- Q. Xu, S. Tao, Q. Jiang and D. Jiang, Ion Conduction in Polyelectrolyte Covalent Organic Frameworks, *J. Am. Chem. Soc.*, 2018, **140**, 7429–7432.
- G. Zhang, Y.-L. Hong, Y. Nishiyama, S. Bai, S. Kitagawa and S. Horike, Accumulation of Glassy Poly(ethylene oxide) Anchored in a Covalent Organic Framework as a Solid-State Li<sup>+</sup> Electrolyte, *J. Am. Chem. Soc.*, 2019, **141**, 1227–1234.
- Y. Wang, K. Zhang, X. Jiang, Z. Liu, S. Bian, Y. Pan, Z. Shan, M. Wu, B. Xu and G. Zhang, Branched Poly(ethylene glycol)-Functionalized Covalent Organic Frameworks as Solid Electrolytes, *ACS Appl. Energy Mater.*, 2021, **4**, 11720–11725.
- S. Tamura, M. Yamane, Y. Hoshino and N. Imanaka, Highly conducting divalent Mg<sup>2+</sup> cation solid electrolytes with well-ordered three-dimensional network structure, *J. Solid State Chem.*, 2016, **235**, 7–11.

